Excitation energy transfer between closely spaced multichromophoric systems

Didraga, Catalin; Malyshev, V.A.; Knoester, Jasper

Published in:
Journal of Physical Chemistry B

DOI:
10.1021/jp0569281

Publication date:
2006

Excitation Energy Transfer between Closely Spaced Multichromophoric Systems: Effects of Band Mixing and Intraband Relaxation†

C. Didraga, V. A. Malyshev,‡ and J. Knoester*

Institute for Theoretical Physics and Materials Science Centre, University of Groningen, Nijenborgh 4, 9747 AG Groningen, The Netherlands

Received: November 29, 2005; In Final Form: April 5, 2006

We theoretically analyze the excitation energy transfer between two closely spaced linear molecular *J*-aggregates, whose excited states are Frenkel excitons. The aggregate with the higher (lower) exciton band edge energy is considered as the donor (acceptor). The celebrated theory of Förster resonance energy transfer (FRET), which relates the transfer rate to the overlap integral of optical spectra, fails in this situation. We point out that, in addition to the well-known fact that the point-dipole approximation breaks down (enabling energy transfer between optically forbidden states), also the perturbative treatment of the electronic interactions between donor and acceptor system, which underlies the Förster approach, in general loses its validity due to overlap of the exciton bands. We therefore propose a nonperturbative method, in which donor and acceptor bands are mixed and the energy transfer is described in terms of a phonon-assisted energy relaxation process between the two new (renormalized) bands. The validity of the conventional perturbative approach is investigated by comparing to the nonperturbative one; in general, this validity improves for lower temperature and larger distances (weaker interactions) between the aggregates. We also demonstrate that the interference between intraband relaxation and energy transfer renders the proper definition of the transfer rate and its evaluation from experiment a complicated issue that involves the initial excitation condition. Our results suggest that the best way of determining this transfer rate between two *J*-aggregates is to measure the fluorescence kinetics of the acceptor *J*-band after resonant excitation of the donor *J*-band.

I. Introduction

The theory of Förster resonance energy transfer (FRET) between two chromophores (molecules, ions) with dipole-allowed optical transitions,[1] and its generalization by Dexter[2] to forbidden optical transitions and exchange interactions between the chromophores, already have a history of more than 50 years. This celebrated theory gives an excellent description of transfer rates for distant chromophores with rather broad spectral lines.[3−5] It describes these rates in terms of the overlap integral of experimentally measured optical absorption and luminescence spectra, which makes it of great utility. With minor reformulations, the concept of FRET may also be applied successfully to the description of nonradiative transitions in ions and molecules in condensed phases,[6] as well as to energy transfer in the presence of a nonstationary bath relaxation.[7] Finally, it has been shown that the Förster theory also explains the efficient long-range energy transfer in assemblies of closely packed CdSe quantum dots[8−10] and CdSe nanocrystals assembled with molecular wires,[11] systems of possible use for quantum computation.[12,13]

Despite its great success, it has been recognized since the 1980s that, in certain situations, standard FRET theory is not applicable. In particular, this holds for chromophores with narrow spectral lines and a small spectral overlap, such as rare-earth ions embedded in a crystalline or glassy host.[14−17] More recently, another important situation in which FRET theory may break down has been emphasized, namely energy transfer between two systems that both contain many interacting chromophores. This problem has drawn particular attention in the context of excitation energy transfer from the B800 to the B850 ring of the photosynthetic antenna system LH2.[18−24] The first complication when dealing with systems of strongly interacting chromophores is that their excited states are excitons, consisting of a coherent superposition of the excited states of many molecules. Because of their spatial extent, which may easily exceed the separation between the two systems, the effective interaction between an exciton state on the donor system and one on the acceptor system cannot be modeled as the interaction between the transition dipoles of both states. As a result, excitation energy transfer may occur from or toward a dipole-forbidden (optically dark) exciton state, implying that a description of the energy transfer in terms of overlap integrals of optical spectra no longer holds. This breakdown of the point-dipole approximation was first pointed out by Sumi and co-workers.[18,19] Treating the electronic coupling between both rings in LH2 as a perturbation, they derived a transfer rate between the rings that strongly differed in magnitude from the Förster result and that was in good agreement with experiment.[25,26]

It should be noted that LH2 is a rather special case of transfer between two aggregates. The reason is that the molecules in the B800 ring are weakly coupled to each other. Thus, the B800 excitations are almost monomeric,[27] and they occur in a narrow band just above the upper edge of the B850 band and far (965 cm^{-1}) away from the optically dominant bottom of that band.[19,28] Moreover, the intermolecular interactions between both rings are weak, on the order of 20 cm^{-1}.[28] Given these special

† Part of the special issue "Robert J. Silbey Festschrift".

* Corresponding author. E-mail: j.knoester@rug.nl. Fax: 31-50-3634947.

‡ On leave from S. I. Vavilov State Optical Institute, Birzhevaya Liniya 12, 199034 Saint-Petersburg, Russia.

10.1021/jp0569281 CCC: $33.50
Published on Web 06/21/2006

circumstances, it is not surprising that the perturbative treatment of the interaggregate (inter-ring) interactions gives good results.

In many cases of closely separated aggregates, however, a perturbative treatment of the interaction that causes energy transfer between them will not be valid. An interesting example is the case of nanotubular carbocyanine *J*-aggregates that have recently been developed by Dähne and co-workers[29−31] and which have been suggested as building blocks for synthetic light-harvesting systems. These aggregates consist of two walls, which are only a few nanometers apart. Each wall is responsible for the formation of an exciton band; even though their optically dominant lower edges are separated by a few hundred cm^{-1}, the two bands overlap over a large energy range (∼2000 cm^{-1}).[32] By using fluorescence and pump−probe experiments, fast excitation energy transfer between both walls has been observed.[33] The strong overlap of the exciton bands makes it doubtful that a perturbative treatment of the interwall interactions holds for this example: (dark) states inside both bands may be close to degenerate, thus falling outside the perturbative regime. This observation also holds for the example of energy transfer between two linear pseudoisocyanine aggregates studied by Kobayashi and co-workers.[34] Like Sumi and co-workers, these authors focused on a breakdown of the dipole approximation; they did not consider the limitations of a perturbative treatment.

The aim of this paper is to study theoretically the energy transfer between two molecular *J*-aggregates carrying Frenkel excitons. We will be inspired by the example of the double-wall cyanine tubes, where the bottoms of both exciton bands occur at different energies, but their central parts overlap. To keep the problem computationally tractable, we will consider two interacting linear *J*-aggregates with different bandwidths, leading to a crossing of both bands in their center. The chain with the higher (lower) band bottom is considered the donor (acceptor). By using this generic model, we will investigate the breakdown of the perturbative approach by comparing to an exact treatment in which both aggregates form one exciton system and the energy transfer is associated with phonon-assisted relaxation within this system. We thus find that the crossover between the weak coupling (perturbative) and strong coupling (nonperturbative) situations is determined by the separation between both aggregates as well as by the temperature.

Another important issue that we address is that fast intraband relaxation (thermalization) between visible and dark exciton states may obscure the observation of the actual energy transfer process and thereby plays a crucial role in the proper definition of the transfer rate as extracted from experiment. As a consequence, also the initial excitation conditions strongly affect the possibility to measure the transfer rate. This key role of intraband relaxation in the process of energy transfer between excitonic systems seems to have gone unnoticed thus far.

The outline of this paper is as follows. In Section II, we first present our model of two homogeneous linear *J*-aggregates, interacting with each other as well as with a vibrational bath. We then introduce the general issue of perturbative versus nonperturbative treatment of interchain interactions by considering the various dynamic processes that can occur in and between weakly coupled or strongly mixed exciton bands. The perturbative approach is worked out in more detail in Section III, where we derive the general expression for the one-phonon assisted transfer rate between any two exciton states located on different chains. In Section IV, we develop the approach for the case of strong interchain coupling (nonperturbative case). Results of numerical simulations of the fluorescence kinetics in both the perturbative and the nonperturbative approach are presented in Section V and are used to study the validity of the former as well as the best way to extract the transfer rate from experiment. Both the temperature and distance dependence of the transfer dynamics are addressed and distinction is made between resonant and off-resonant initial excitation of the donor. A comparison to standard FRET theory is made as well. Finally, in Section VI, we summarize.

II. Model and General Strategy

A. Model. We consider two parallel linear chains, each consisting of N equidistant two-level chromophores, with their transition dipoles aligned to the chains (see Figure 1). The lattice spacing within each chain is denoted h, while the distance between the chains is d. One of the chains will be referred to as the donor (D), the other as the acceptor (A) (see below). We will assume that both chains are homogeneous, and we will impose periodic boundary conditions in the chain direction (the formalism may easily be extended to account for disorder and open boundary conditions). The chromophores building up the D chain are different from those of the A chain; in particular, we will assume that the transition energies and dipoles of the individual chromophores within the D chain all have the values ϵ_D and μ_D, respectively, while in the A chain, they take the values ϵ_A and μ_A. We will account for the dipole−dipole interactions between all chromophores in both chains and also include in the model a coupling of the electronic excitations to a bath of vibrations. The latter coupling is derived from the first-order change of the chromophores' transition energies caused by nuclear displacements in the environment. In the site representation, the resulting Hamiltonian of system and bath reads

$$H = H_D + H_A + H_{DA} + H_{bath} + H_{D-bath} + H_{A-bath} \quad (1)$$

with

$$H_D = \epsilon_D \sum_{n=1}^{N} |n, D\rangle\langle n, D| + \sum_{n,m=1}^{N} J_{nm}^{D} |n, D\rangle\langle m, D| \quad (2a)$$

$$H_A = \epsilon_A \sum_{n=1}^{N} |n, A\rangle\langle n, A| + \sum_{n,m=1}^{N} J_{nm}^{A} |n, A\rangle\langle m, A| \quad (2b)$$

$$H_{DA} = \sum_{n,m=1}^{N} J_{nm}^{DA} |n, D\rangle\langle m, A| + h.c. \quad (2c)$$

$$H_{bath} = \sum_{q} \omega_q a_q^{\dagger} a_q \quad (2d)$$

$$H_{D-bath} = \sum_{n=1}^{N} \sum_{q} V_{nq}^{D} |n, D\rangle\langle n, D|\, a_q + h.c. \quad (2e)$$

$$H_{A-bath} = \sum_{n=1}^{N} \sum_{q} V_{nq}^{A} |n, A\rangle\langle n, A|\, a_q + h.c. \quad (2f)$$

Here, H_D and H_A denote the electronic (exciton) Hamiltonians for the isolated donor and acceptor chains, respectively, while H_{DA} is the electronic interaction between both chains, composed of all dipole−dipole interactions between molecules of one chain and the other. In these terms, $|n, D\rangle$ ($|n, A\rangle$) denotes the state in which the nth ($n = 1, ..., N$) chromophore of the donor (acceptor) chain is excited and all the other chromophores are in the ground state. Furthermore, the hopping integrals J_{nm}^{D},

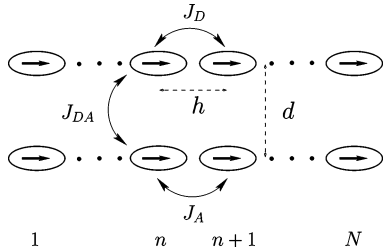

Figure 1. The two linear *J*-aggregates (D and A) considered in this paper. Both chains contain *N* chromophores, labeled *n*, which interact with each other through their transition dipoles (indicated by arrows). The scale of the interactions is set by the quantities J_D, J_A, and J_{DA}, which give the interactions between the various pairs of nearest neighbors. The lattice spacing within each chain is denoted *h*, while the interchain distance is given by *d*.

J^{A}_{nm}, and J^{DA}_{nm} are the various dipole−dipole interaction matrix elements between chromophores of the same or different chains. For the geometry considered here, we have $J^{D}_{nm} = -J_D/|n-m|^3$, $J^{A}_{nm} = -J_A/|n-m|^3$, $J^{D}_{nn} = J^{A}_{nn} = 0$, and $J^{DA}_{nm} = J_{DA}[1-2(n-m)^2h^2/d^2]/[1+(n-m)^2h^2/d^2]^{5/2}$, with $J_D \equiv 2\mu_D^2/h^3$, $J_A \equiv 2\mu_A^2/h^3$, and $J_{DA} \equiv \mu_D\mu_A/d^3$.

H_{bath} describes the vibrational modes of the host, labeled *q* and with the energy spectrum ω_q (we set $\hbar = 1$). The operator *a* annihilates a vibrational quantum in mode *q*. Finally, H_{D-bath} and H_{A-bath} represent the operators of the exciton−bath coupling of the donor and acceptor, respectively, where the quantities V^{D}_{nq} and V^{A}_{nq} indicate their strength. We do not provide explicit expressions for these quantities; rather we will consider them on a phenomenological basis. Specifically, realizing that, in most experimental studies of aggregates, the host is strongly disordered, we will treat these strengths as stochastic variables with correlation properties:

$$\langle V^{D}_{nq}\rangle = \langle V^{A}_{nq}\rangle = \langle V^{D}_{nq}\, V^{A*}_{mq}\rangle = 0 \tag{3a}$$

$$\langle V^{D}_{nq}\, V^{D*}_{mq}\rangle = \delta_{nm}|V^{D}_{q}|^2 \tag{3b}$$

$$\langle V^{A}_{nq}\, V^{A*}_{mq}\rangle = \delta_{nm}|V^{A}_{q}|^2 \tag{3c}$$

These relations imply that the surroundings of different chromophores are not correlated.

B. Strategy. We now turn to a general discussion of a perturbative versus nonperturbative approach to describe the excitation energy transfer between both chains. Throughout this paper, we will assume that the exciton−phonon coupling is weak compared to the intrachain dipole−dipole interactions, in the sense that the coherence length of the excitons within each chain is not limited by the coupling to the bath. In that case, the Bloch eigenstates of H_D and H_A are a good starting point for our considerations, and the main role of the bath is to make up for energy differences in possible intraband energy relaxation. The Bloch states read (X = D, A)

$$|k, X\rangle = \sum_{n=1}^{N} \varphi^{X}_{kn}|n, X\rangle = \frac{1}{\sqrt{N}}\sum_{n=1}^{N} \exp\left[\frac{2\pi i k n}{N}\right]\Big|n, X\Big\rangle \tag{4}$$

with energy

$$E^{X}_{k} = \epsilon_X - 2J_X\sum_{n=1}^{N/2}\frac{1}{n^3}\cos\left[\frac{2\pi i k n}{N}\right] \tag{5}$$

Here, *k* is the wavenumber of the state, which can take the values 0, 1, ..., $N-1$.

Figure 2a shows the donor and the acceptor bands, E^{D}_{k} and E^{A}_{k}, respectively, for chains of $N = 150$ molecules, with $\epsilon_D = \epsilon_A$ (we take this as zero of energy) and $J_A = 1.14J_D$. Only half of the Brillouin zone is plotted, as the dispersion relation is symmetric around $k = N/2$. We see two exciton bands that cross at their center. The bottom of each band occurs at $k = 0$, which is the superradiant state that contains all oscillator strength to the ground state; all other exciton states are optically forbidden. Thus, as long as the interactions between the chains are weak, the fluorescence spectrum consists if two *J*-bands, whose positions are indicated by the dots on the $k = 0$ axis. By definition, we choose our labeling such that $E^{D}_{k=0} > E^{A}_{k=0}$. The energy separation between both peaks will be denoted Δ and is (for $N \gg 1$) given by $\Delta = \epsilon_D - \epsilon_A + 2\zeta(3)(J_A - J_D)$, with $\zeta(x)$ the Riemann zeta function.

The two chains are coupled electronically by the interaction H_{DA} (eq 2c), which on the basis of Bloch states is diagonal, i.e., $H_{DA} = \sum_k J^{DA}_{kk}|k, D\rangle\langle k, A| + h.c.$, with

$$J^{DA}_{kk} = J_{DA} + 2J_{DA}\sum_{n=1}^{N/2}\frac{1-2(nh/d)^2}{[1+(nh/d)^2]^{5/2}}\cos\left(\frac{2\pi k n}{N}\right) \tag{6}$$

In general, this expression must be evaluated numerically (see Figure 2c for an example). Only in the limiting (and rather unphysical) case of $d \ll h$ it is easily seen that $J^{DA}_{kk} = J_{DA} = \mu_D\mu_A/d^3$, independent of *k*.

As long as the interactions J^{DA}_{kk} are weak (large separation *d*), it seems reasonable to apply the usual perturbative approach to them by using the bands of the isolated donor and acceptor chains as starting point. We will follow this route in Section III, where we also will treat the exciton−phonon interactions perturbatively. In this approach, the rate of energy transfer between an arbitrary donor state and acceptor state is calculated using second-order perturbation theory, involving two steps: (i) The excitation is transferred from the donor to the acceptor; (ii) A phonon-induced scattering occurs within the acceptor band (scattering within the donor followed by transfer to the acceptor is possible as well). The overall process should conserve the total energy. Both steps are schematically indicated in Figure 2b, in which we zoomed in on the small-*k* part of the bands given in Figure 2a. Because in our example the interchain interaction is diagonal in *k*, the transfer step is a vertical transition between both bands. We notice that, aside from energy transfer between both chains, the interactions with the phonon bath also give rise to relaxation of the exciton states within both bands; details of this process are studied in ref 36.

If we focus on the optically dominant bottom states of both bands, it seems that the perturbative treatment of the interchain interactions is valid as long as $|J^{DA}_{k=0,k=0}| \ll \Delta$. Generally speaking, this criterion is not sufficient, however. Depending on temperature and initial excitation condition, the transfer process may involve the optically forbidden states higher in the exciton bands. As near the band center the donor and acceptor states get arbitrarily close in energy, a perturbative approach necessarily fails there. For this situation, one has to resort to a nonperturbative treatment in which both bands are mixed. As long as $|J^{DA}_{k=0,k=0}| \ll \Delta$, the amount of mixing will be weak for the superradiant band bottoms, but strong near the center.

For our case of translational symmetry, the mixed eigenstates of $H_D + H_A + H_{DA}$ read (see, e.g., ref 37)

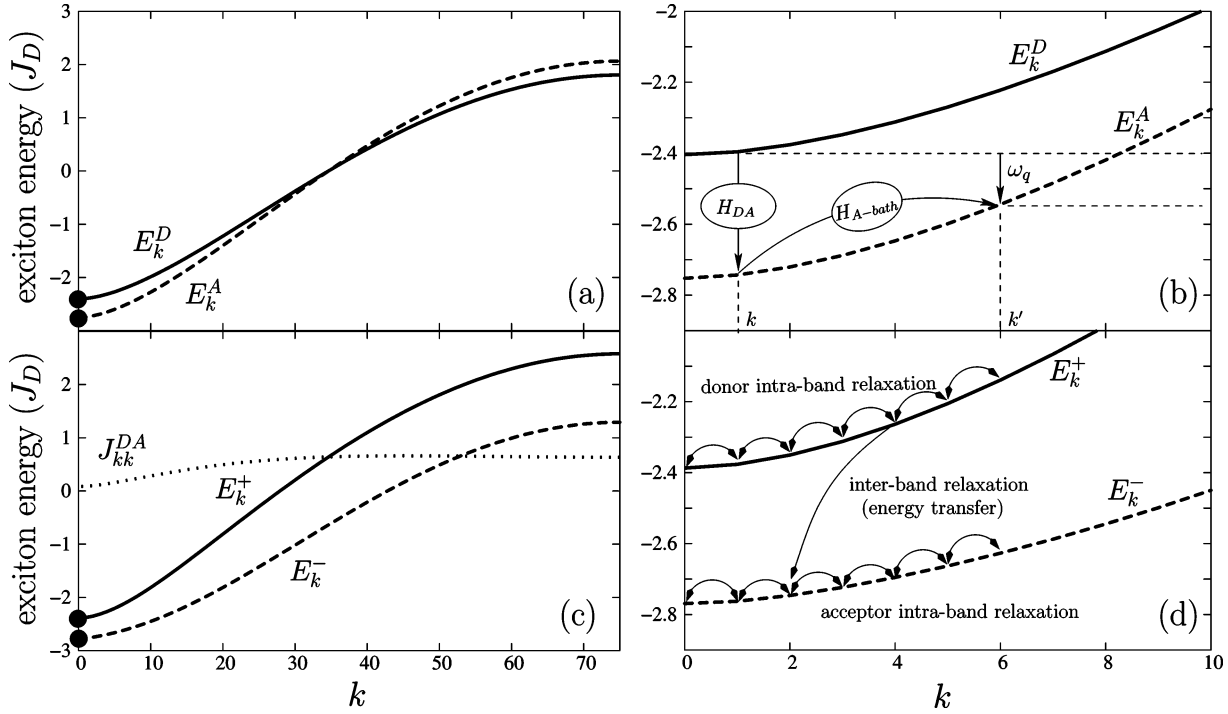

Figure 2. (a) Exciton bands for donor (solid) and acceptor (dashed) chains of $N = 150$ molecules in the absence of interchain coupling for the case $J_A = 1.14J_D$ and setting $\epsilon_A = \epsilon_D = 0$. Note that we have only plotted half of the Brillouin zone, as it is symmetric with respect to $k = N/2$. The dots at $k = 0$ indicate the positions of the absorption peaks of donor and acceptor band, respectively. (b) Enlarged view of the small-k part of panel (a), with schematic indication of the two-step perturbative view of the interchain energy transfer described in the text. (c) Exciton bands for the same system as in panel (a), but now after accounting for the mixing between the eigenstates of both chains due to the interchain interaction with strength $J_{DA} = 0.535J_D$ (corresponding to an interchain separation $d = h$.) The k-dependence of the interchain coupling J_{kk}^{DA} is depicted as well. (d) Enlarged view of the small-k part of the panel (c), with schematic indication of the various phonon-assisted intraband and interband relaxation processes that together are responsible for the exciton dynamics within the nonperturbative picture.

$$|k,\pm\rangle = \frac{1}{\sqrt{2}}\left[\left(1 \pm \frac{1}{\sqrt{1+\eta_k}}\right)^{1/2}\left|k, \mathrm{D}\right\rangle \pm \left(1 \mp \frac{1}{\sqrt{1+\eta_k}}\right)^{1/2}\left|k, \mathrm{A}\right\rangle\right] \quad (7a)$$

with energies

$$E_k^{\pm} = \frac{1}{2}(E_k^{\mathrm{D}} + E_k^{\mathrm{A}}) \pm \frac{1}{2}(E_k^{\mathrm{D}} - E_k^{\mathrm{A}})\sqrt{1+\eta_k} \quad (7b)$$

Here, $\pm$ labels the new (decoupled) exciton bands and $\eta_k = 4|J_{kk}^{\mathrm{DA}}|^2/(E_k^{\mathrm{D}} - E_k^{\mathrm{A}})^2$ is the quantity that characterizes the amount of mixing at wavenumber k. The new bands are plotted in Figure 2c for the same parameters as in Figure 2a, accounting for an interchain interaction of strength $J_{\mathrm{DA}} = 0.535J_{\mathrm{D}}$ (which corresponds to a small interchain separation of $d = h$). The coupling J_{kk}^{DA} is depicted as well. As we see, at the band bottoms, the coupling is very small compared to Δ and the states are hardly mixed ($\eta_{k=0} = 0.2$). Hence, we may still refer to the fluorescence coming from the bottom of the upper (lower) band as the donor (acceptor) fluorescence. At the center of the bands, the mixing is very strong and a band anticrossing occurs. Also after mixing, the only states with oscillator strength occur at the band bottoms.

After accounting for the band mixing, the only remaining dynamics that can take place is phonon-assisted scattering of the new exciton states, leading to intraband and interband relaxation of the excitation energy (see processes indicated in Figure 2d). In Section IV, this approach will be further specified, using the Fermi golden rule to account for the exciton−phonon interaction.

To end this section, we stress that the special conditions imposed in our model, such as chains of equal length and periodicity, periodic boundary conditions, and the absence of disorder in the electronic part of the Hamiltonian, may be relaxed without affecting the above formalism and the distinction between the perturbative and nonperturbative approach. In fact, in all expressions presented in Sections III and IV, we will use a general notation for the exciton wave functions, $\varphi_{kn}^{\mathrm{D}}$, $\varphi_{kn}^{\mathrm{A}}$, and $\phi_{\nu n}$, so that these expressions keep their validity under generalized conditions, as long as the proper exciton eigenfunctions of the generalized H_{D}, H_{A}, and $H_{\mathrm{D}} + H_{\mathrm{A}} + H_{\mathrm{DA}}$ are used as input. In that case, k and ν refer to the appropriate quantum numbers, which do not necessarily have the meaning of quasimomenta.

III. Perturbative Approach

In this section, we follow the perturbative approach outlined in Section II.B. In this approach, the Hamiltonian of the unperturbed system reads $H_0 = H_{\mathrm{D}} + H_{\mathrm{A}} + H_{\mathrm{bath}}$, while $H' = H_{\mathrm{DA}} + H_{\mathrm{D-bath}} + H_{\mathrm{A-bath}}$ represents the perturbation that induces transitions between the eigenstates of H_0. On the basis of exciton eigenstates of the noninteracting chains (eq 4), the interchain coupling and the exciton−bath interactions take the form

$$H_{\mathrm{DA}} = \sum_{k,k'=1}^{N} J_{kk'}^{\mathrm{DA}}|k, \mathrm{D}\rangle\langle k', \mathrm{A}| + h.c. \quad (8a)$$

with $J_{kk'}^{\mathrm{DA}} = \sum_{n,m} J_{nm}^{\mathrm{DA}}\varphi_{kn}^{\mathrm{D}}\varphi_{k'm}^{\mathrm{A}*}$ and

$$H_{\mathrm{X-bath}} = \sum_{k,k'=1}^{N}\sum_{q} V_{kk'q}^{\mathrm{X}}|k, \mathrm{X}\rangle\langle k', \mathrm{X}|\, a_q + h.c. \quad (8b)$$

with $V^{X}_{kk'q} = \sum_n V^{X}_{nq} \varphi^{X*}_{kn} \varphi^{X}_{k'n}$ and X = D, A.

We aim to consider the energy transfer between any donor state $|k, D\rangle$ and any acceptor state $|k', A\rangle$. Because the transfer operator H' does not produce such transitions within first-order perturbation theory, we have to resort to the second-order term. The corresponding expression for the transfer rate reads

$$W_{k'A,kD} = 2\pi \sum_f \sum_i \rho(E_i) \left\langle \left| \sum_s \frac{\langle f|H'|s\rangle\langle s|H'|i\rangle}{E_i - E_s} \right|^2 \right\rangle \times \delta(E_f - E_i) \quad (9)$$

Here, $|i\rangle = |k, D\rangle|\{n_q\}_i\rangle$ and $|f\rangle = |k', A\rangle|\{n_q\}_f\rangle$ are the initial and final states, respectively, where $\{n_q\}$ denotes the set of occupation numbers of the vibrational modes. $E_i = E^{D}_k + \Omega_i$ and $E_f = E^{A}_{k'} + \Omega_f$ are the corresponding energies, with Ω_i and Ω_f denoting the energies of the bath in the initial and final states, respectively. Furthermore, s labels the intermediate states $|s\rangle$, with energies E_s and the quantity $\rho(E_i)$ is the equilibrium density matrix of the bath's initial state. Finally, the angular brackets indicate that we average over the stochastic realizations of the surroundings of donor and acceptor chromophores.

By evaluating the expressions in eq 9 and accounting for the stochastic properties of the exciton−bath couplings (eqs 3), we obtain

$$W_{k'A,kD} = \mathscr{D}(|E^{D}_k - E^{A}_{k'}|) \left[\sum_{k''} \frac{|J^{DA}_{k'k''}|^2}{(E^{A}_{k'} - E^{D}_{k''})^2} \mathscr{O}^{D}_{k''k} + \sum_{k''} \mathscr{O}^{A}_{k'k''} \frac{|J^{DA}_{k''k}|^2}{(E^{D}_k - E^{A}_{k''})^2} \right] \times \begin{cases} 1 + \bar{n}, (E^{D}_k - E^{A}_{k'}), & E^{D}_k > E^{A}_{k'} \\ \bar{n}(E^{A}_{k'} - E^{D}_k), & E^{D}_k < E^{A}_{k'} \end{cases} \quad (10)$$

where $\mathscr{D}(\omega)$ is the vibration spectral density of the bath, which we assume to be identical for the donor and acceptor. It is given by

$$\mathscr{D}(\omega) = 2\pi \sum_q |V^{X}_q|^2 \delta(\omega - \omega_q) \quad (11)$$

where X = D, A. The quantity $\mathscr{O}^{X}_{kk'}$ denotes the probability overlap of the donor states $|k, D\rangle$ and $|k', D\rangle$ for X = D and of the acceptor states $|k, A\rangle$ and $|k', A\rangle$ for X = A:

$$\mathscr{O}^{X}_{kk'} = \sum_{n=1}^{N} |\varphi^{X}_{kn}|^2 |\varphi^{X}_{k'n}|^2 \quad (12)$$

Finally, $\bar{n}(\omega_q) = [\exp(\omega_q/T) - 1]^{-1}$ is the mean occupation number of the vibrational mode q (the Boltzmann constant $k_B = 1$).

The transfer rate, eq 10, reflects the two-step processes introduced in Section II.B. The first term corresponds to the process in which the initial exciton of wavenumber k on the donor chain is scattered into the exciton state k'' on the donor under the creation or annihilation of a phonon q, followed by the transfer of the exciton k'' to an exciton k' on the acceptor chain. Likewise, the second term in eq 10 derives from the process, in which the donor's initial exciton k is first transferred to the acceptor chain k'', followed by a phonon-induced scattering to the final acceptor state k'.

Equation 10 clearly indicates that, in general, the energy transfer may occur between any pair of donor and acceptor states, independently of whether those states are optically allowed or forbidden: neither the probability overlap $\mathscr{O}^{X}_{kk'}$ nor the transfer interactions $J^{DA}_{kk'}$ vanish for general k and k'. Equation 10 reduces to Förster's formula only if the distance d between the chains is larger than their lengths Nh. Indeed, in that case, the interchain interactions are well-approximated by $J^{DA}_{kk'} = (\mu_D \mu_A / d^3) \sum_{n=1}^{N} \varphi^{D*}_{kn} \sum_{m=1}^{N} \varphi^{A}_{k'm}$, where the sums correspond to the dimensionless transition dipole moments of the states $|k, D\rangle$ and $|k', A\rangle$. For our ordered chains, these dipole moments are giant for $k = k' = 0$, while they vanish for all other states. Thus, the term $J^{DA}_{k=0,k'=0}$ is dominant. The energy transfer between the chains may then be viewed as Förster-type due to the overlap of the donor's sideband fluorescence and the zero-phonon acceptor absorption and vice versa.

The importance of the forbidden exciton states in the energy transfer between excitonic systems was mentioned for the first time by Sumi and co-workers[18,19] and later on received attention from several authors.[20−24,34] We note that, in refs 18 and 19, the problem was treated in a more general way than we did above: only the transfer interactions J^{DA}_{nm} were considered as perturbations, while the exciton−bath couplings were accounted for by a self-consistent second-order evaluation of the self-energy. We do not use such a self-consistent treatment of the exciton−bath interaction in this paper, as it turns out that it is impossible to combine it with the nonperturbative treatment of the transfer interactions, which we will investigate in the next section.

The expression for $W_{k'A,kD}$ obtained above allows one to calculate the energy transfer rate between any pair of donor and acceptor states. From the occurrence of the energy denominators in eq 10, however, it is clear that the perturbative approach of the interchain interactions is restricted to situations where the donor and acceptor bands do not cross. A band crossing or (for disordered systems) a band overlap will lead to small denominators, breaking the result of perturbation theory and giving rise to rates that are large compared to the energy spacing of the states involved. This motivates the nonperturbative approach presented in the next section.

IV. Nonperturbative Approach

In this section, we work out in more detail the nonperturbative approach outlined in Section II.B, in which the interchain interactions are accounted for exactly through mixing of the exciton bands of the isolated chains. We will label the $2N$ mixed eigenstates of $H_{ex} = H_D + H_A + H_{DA}$ with a Greek index $\nu = 1, ..., 2N$; they take the form

$$|\nu\rangle = \sum_{n=1}^{2N} \phi_{\nu n} |n\rangle \quad (13)$$

where $|n\rangle = |n, D\rangle$ for $n = 1, ..., N$ and $|n\rangle = |n - N, A\rangle$ for $n = N + 1, ..., 2N$. The corresponding energy is denoted E_ν. For the special highly symmetric model considered in this paper, the explicit forms of the eigenstates and energies have been given in Section II.B already, where the ν index should be identified with the $k\pm$ labeling. In the current section, the notation is kept general.

In the new representation, the exciton−bath coupling, which is the perturbation that causes the exciton dynamics, reads

$$H_{D-bath} + H_{A-bath} = \sum_{\mu,\nu=1}^{2N} \sum_q V_{\mu\nu q} |\mu\rangle\langle\nu| a_q + h.c. \quad (14)$$

with $V_{\mu\nu q} = \sum_{n=1}^{2N} V_{nq} \phi^*_{\mu n} \phi_{\nu n}$, where, as before, the coupling

strength V_{nq} is considered a stochastic function of the site index n with properties similar to those given by eqs 3: $\langle V_{nq}\rangle = 0$ and $\langle V_{mq}V_{nq}^*\rangle = \delta_{mn}|V_q|^2$.

As discussed in Section II.B, the dynamics of the excitons in the new representation is caused by their scattering on phonons. To describe this process, we will use a Pauli master equation for the populations $P_\nu(t)$ of the exciton states:

$$\dot{P}_\nu = -\gamma_\nu P_\nu + \sum_\mu (W_{\nu\mu}P_\mu - W_{\mu\nu}P_\nu) \tag{15}$$

Here, $\gamma_\nu = \gamma_0 F_\nu$ is the radiative decay rate of the state $|\nu\rangle$, where γ_0 is this rate for a single chromophore (for simplicity, taken identical for donor and acceptor) and $F_\nu = |\sum_{n=1}^{2N}\phi_{\nu n}|^2$ denotes the dimensionless oscillator strength of the exciton. Furthermore, the scattering rates $W_{\mu\nu}$ are obtained by using Fermi's golden rule, taking into account the stochastic properties of the exciton−bath coupling strength V_{qn}. They are given by[35,36]

$$W_{\mu\nu} = \mathscr{D}(|E_\mu - E_\nu|)\mathscr{O}_{\mu\nu} \times \begin{cases} 1+\bar{n}(E_\nu - E_\mu), & E_\nu > E_\mu \\ \bar{n}(E_\mu - E_\nu), & E_\mu > E_\nu \end{cases} \tag{16}$$

where $\mathscr{D}(\omega)$ is the spectral density of the bath, given by eq 11 with V_q^X replaced by V_q. Furthermore, $\mathscr{O}_{\mu\nu}$ is the probability overlap of states μ and ν,

$$\mathscr{O}_{\mu\nu} = \sum_{n=1}^{2N} |\phi_{\mu n}|^2|\phi_{\nu n}|^2 \tag{17}$$

The explicit expression for $\mathscr{O}_{\mu\nu}$ in the case of homogeneous chains of equal length is given in the Appendix.

To end this section, we note that, in general, the best way to probe the excitation energy transfer is to follow the fluorescence kinetics of donor and acceptor. Even if we allow for inhomogeneity, two coupled aggregates with a clear separation between their individual *J*-bands will lead to a mixed system that still has two *J*-bands, possibly renormalized in magnitude and shifted somewhat (see Figure 2 for the special case of ordered chains). In terms of the energies of the mixed eigenstates and the solution to the Pauli master equation, the time-dependent fluorescence spectrum reads

$$I(E,t) = \langle \sum_\nu \gamma_\nu P_\nu(t)\,\delta(E - E_\nu)\rangle \tag{18}$$

where the brackets denote the average over disorder, if present. One may then define the total donor (acceptor) fluorescence as the integral over the highest (lowest) peak in the spectrum. These two quantities will be analyzed in Section V as a function of time following some initial excitation of the donor chain.

V. Results and Discussion

We now apply the formalism developed in the previous sections to study the energy transfer rates and fluorescence kinetics for the model introduced in Section II, namely two parallel homogeneous chains of N chromophores with periodic boundary conditions. In all examples, we will choose $N = 150$, $\epsilon_A = \epsilon_D$, and $J_A = 1.14J_D$, which implies that $\mu_A = 1.07\mu_D$; the value of J_{DA} depends on the interchain distance d, which we will vary. Given the above parameters, we have $J_{DA} = (\mu_A/\mu_D)(h/d)^3J_D/2 = 0.535(h/d)^3J_D$.

For the spectral density of the bath, we choose

$$D(\omega) = W_0\frac{\omega}{\omega_c}\exp\left(-\frac{\omega}{\omega_c}\right) \tag{19}$$

which represents a model function with Ohmic (i.e., linear) behavior[38] for frequencies up to a cutoff frequency ω_c. The overall prefactor W_0 is a measure of the exciton scattering amplitude imposed by the phonons. A spectral density similar to eq 19, with ω_c on the order of 100 cm^{-1}, has been used successfully to fit the optical dynamics in photosynthetic antenna complexes.[39−42] Also, eq 19 without a cutoff has been used to explain the optical dynamics of aggregates of the dye 3,3′-bis-(sulfopropyl)-5,5′-dichloro-9-ethylthiacarbo-cyanine (THIATS) measured between 0 and 100 K.[43] In the remainder of this paper, we will use $\omega_c = 0.2J_D$, which is reasonable for *J*-aggregates, where J_D typically lies in the range 500−1000 cm^{-1}. W_0 and J_D will be kept arbitrary, where W_0^{-1} will serve as unit of time and J_D as unit of temperature. For example, for $J_D = 800$ cm^{-1}, the choice $T/J_D = 0.25$ agrees with room temperature.

The above specifies all input necessary to determine the transfer rate $W_{k'A,kD}$ (eq 10) between arbitrary states in the perturbative approach, as well as the relaxation rates $W_{\mu\nu}$ (eq 16) in the nonperturbative treatment. In the latter case, the transfer from the donor to the acceptor involves the relaxation rate $W_{k'-,k+}$.

A. Nonperturbative-to-Perturbative Crossover. To assess the validity of the perturbative approach, we calculate the total transfer rate from donor to acceptor chain within both approaches, assuming that the initial exciton populations of the donor manifold are in thermal equilibrium, i.e., we assume that the intraband relaxation is fast compared to the energy transfer process. For the nonperturbative approach, this means that we use as an initial condition $P_{k+}(t=0) = Z_+^{-1}\exp(-E_{k+}/T)$, where $Z_+ = \sum_k \exp(-E_{k+}/T)$, while the acceptor band is not populated, $P_{k-}(t=0) = 0$. Then, the effective quantity

$$W_{-+} = \frac{1}{Z_+}\sum_{k,k'}\exp\left(-\frac{E_{k+}}{T}\right)W_{k'-,k+} \tag{20}$$

may be associated with the energy transfer rate from the donor to the acceptor band at the initial stage of the transfer when the back transfer is negligible. In the perturbative treatment, the analogue of this effective transfer rate is given by

$$W_{AD} = \frac{1}{Z_D}\sum_{k,k'}\exp\left(-\frac{E_k^D}{T}\right)W_{k'A,kD} \tag{21}$$

with $Z_D = \sum_k \exp(-E_k^D/T)$. By construction, $W_{-+} \to W_{AD}$ in the limit of large interchain distance d, i.e., small interchain interactions ($\eta_k \ll 1$).

Figure 3 shows the results of our calculations for W_{-+} (thick lines) and W_{AD} (thin lines) as a function of the interchain distance d. From this figure, it is clearly seen that the perturbative approach strongly overestimates the energy transfer rate for small d, as expected. It is also seen that in the limit of large d, both treatments indeed are in perfect agreement. However, the value of d below which the perturbative approach fails, increases for growing temperature. This finds its natural explanation in the band mixing. Let us first consider the situation at $T = 0$. Then, only relaxation from the donor band edge state $|0+\rangle$ to states in the acceptor band below the donor band edge contribute to W_{-+}. For our choice of parameters, even at distances as small as $d = h$, these states in the vicinity of the band edges are only weakly coupled ($\eta_{k\approx 0}$ is rather small, see

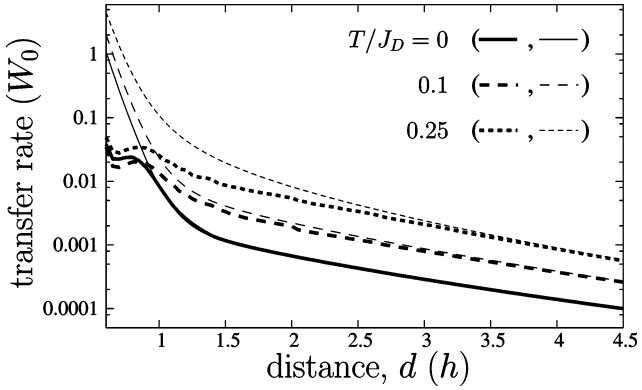

Figure 3. Donor to acceptor energy transfer rate in the nonperturbative approach (thick lines) and the perturbative approach (thin lines) as a function of the interchain distance d for various temperatures T. These rates are given by W_{-+} (eq 20) and W_{AD} (eq 21), respectively. All parameters as given at the beginning of Section V.

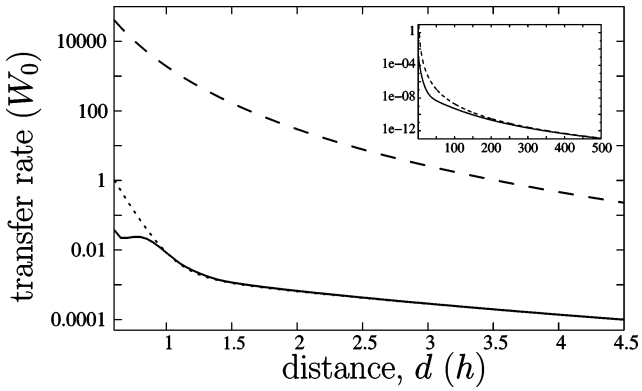

Figure 4. Energy transfer rate as a function of interchain distance at $T = 0$ according to Förster's formula (dashed line, see text for definition) compared to the exact result (solid, eq 20) and the perturbative one (dotted, eq 21). All parameters as given at the beginning of Section V. The inset shows the convergence to Förster's result for very large distances.

Section II.B). This explains why the difference between the perturbative and nonperturbative results quickly vanishes for $d > h$. This difference only is considerable for $d < h$ because the interchain interactions then quickly grow ($\sim 1/d^3$), increasing the band mixing even for the band edge states.

Upon increasing the temperature, the initial population will spread to higher k states in the donor band. For these states, the band mixing becomes increasingly more important, even for growing values of the distance d. This effect finds its origin in the fact that the energy separation between the isolated donor and acceptor bands decreases with growing k, while the interchain interaction J_{kk}^{AD} grows (cf. Figure 2). This explains why the range of d over which the perturbative approach fails increases with growing temperature.

It is of interest also to compare the above-derived energy transfer rates with Förster's formula, which is obtained from eq 21 under the assumption that $J_{kk}^{DA} = (\mu_D \mu_A / d^3)\, N\delta_{k0}$, i.e., by viewing the donor and the acceptor chain as two giant dipoles, irrespective of their separation. Here, we limit ourselves to the rate at $T = 0$, for which Förster's rate reduces to $W_{AD}^{F} = 1911 W_0 (h/d)^6$. This result is plotted as a function of d in Figure 4, together with W_{-+} and W_{AD} at $T = 0$. Clearly, the Förster result gives an enormous overestimation of the exact as well as the perturbative rate for interchain distances smaller than roughly the chain length. This is not surprising because, at distances small compared to the chain size, the $J_{kk'}^{DA}$ defined below eq 8a does not reduce to the interaction between the excitons' transition dipoles.

B. Fluorescence Kinetics. In the above, we characterized the excitation energy transfer by a single rate, which is possible if we assume fast equilibration inside the donor and the acceptor band and neglect the back transfer from the acceptor to the donor. In general, one cannot rely on these assumptions. As we mentioned in Section II.B (also see Section IV), the most straightforward way to characterize the energy transfer between donor and acceptor in experiment is to follow the fluorescence kinetics of both subsystems. In this section, we will use this approach. In all cases, the calculations were done using the nonperturbative method, i.e., accounting for band mixing and for relaxation within and between the mixed bands. We will not assume a priori that equilibration takes place on a time scale shorter than the one for energy transfer. As only the bottom ($k = 0$) states of the mixed bands have oscillator strength, both the absorption and the fluorescence spectrum consist of a single δ peak. Thus, the total donor and acceptor fluorescence intensity as a function of time are given by $I_D(t) = \gamma_{0+} P_{0+}(t)$ and $I_A(t) = \gamma_{0-} P_{0-}(t)$, respectively. These are the quantities that will be analyzed in the following and related to the intraband relaxation and excitation energy transfer.

1. Resonant Excitation. We first study the fluorescence kinetics for resonant excitation, i.e., assuming that initially the superradiant state $|0+\rangle$ of the donor band is excited by the pump. Following this excitation, the population of this state has two channels to relax, namely scattering to higher states in the donor band (intraband relaxation) or scattering to the acceptor band (energy transfer). Once transferred to the acceptor band, the excitation may undergo relaxation within that band, or it may transfer back to the donor. Figure 5 shows the donor fluorescence kinetics $I_D(t)$ resulting from the interplay of these processes at different temperatures and interchain distances, calculated by solving eq 15 with the above initial condition. In doing so, we neglected the radiative decay rates γ_ν of the exciton states, assuming this relaxation channel to be much slower than all the others. As a result, at nonzero temperatures, $P_{0+}(t)$ eventually reaches a finite value, which is in accordance with the Boltzmann equilibrium over donor and acceptor states. We notice that even the neglect of the superradiant emission rate for chains on the order of 100 molecules (10−100 ps lifetime) does not limit the validity of the results presented in this section. Typical values for $1/W_0$ are in the 1−10 fs time scale,[43] so that at all times considered in Figures 5 and 6 the radiative decay indeed has a negligible effect.

In Figure 5b, c, and d, one can distinguish two stages in the donor fluorescence kinetics prior to reaching the Boltzmann equilibrium. These stages are characterized by different time scales. The first stage, indicated by I in Figure 5c, is a fast intraband relaxation. Here, the initially created population of the superradiant donor state $|0, +\rangle$ rapidly scatters to the higher-lying dark states $|k, +\rangle$, resulting in a fast decay of the donor's fluorescence intensity. Obviously, this process gets more pronounced with increasing temperature. The second stage, indicated by II in Figure 5c, is noticeably slower. This stage is associated with the interband relaxation, i.e., with the energy transfer between the donor and acceptor bands. We note that at $T = 0$ the upward intraband relaxation is absent and the monoexponential fluorescence decay directly reflects the transfer rate calculated through eq 20 at $T = 0$.

As is seen, stages I and II are easily separated as long as the interchain distance $d > h$; it is then possible to determine a meaningful effective energy transfer rate from the stage II decay

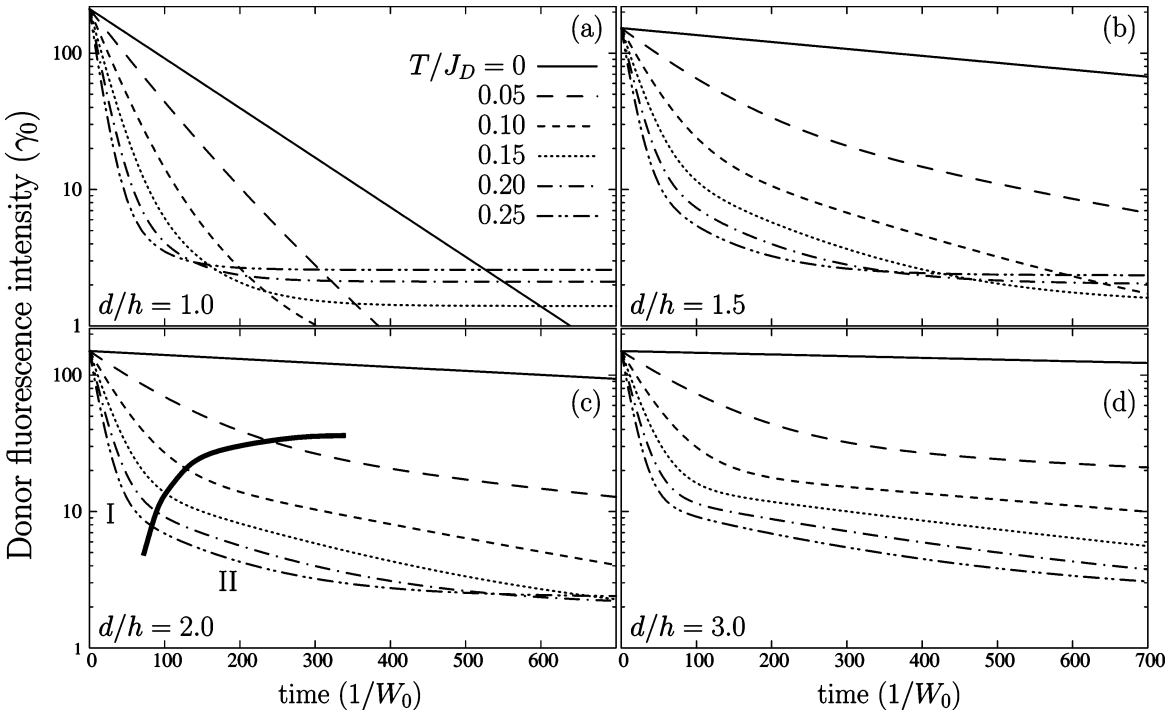

Figure 5. Kinetics of the donor fluorescence $I_D(t)$ following resonant excitation [$P_{k+}(0) = \delta_{k0}$] for different temperatures T and distances d between the chains, as indicated in the panels. All other parameters as given at the beginning of Section V. The thick line in panel (c) separates the two kinetic stages (I and II) distinguished in the text.

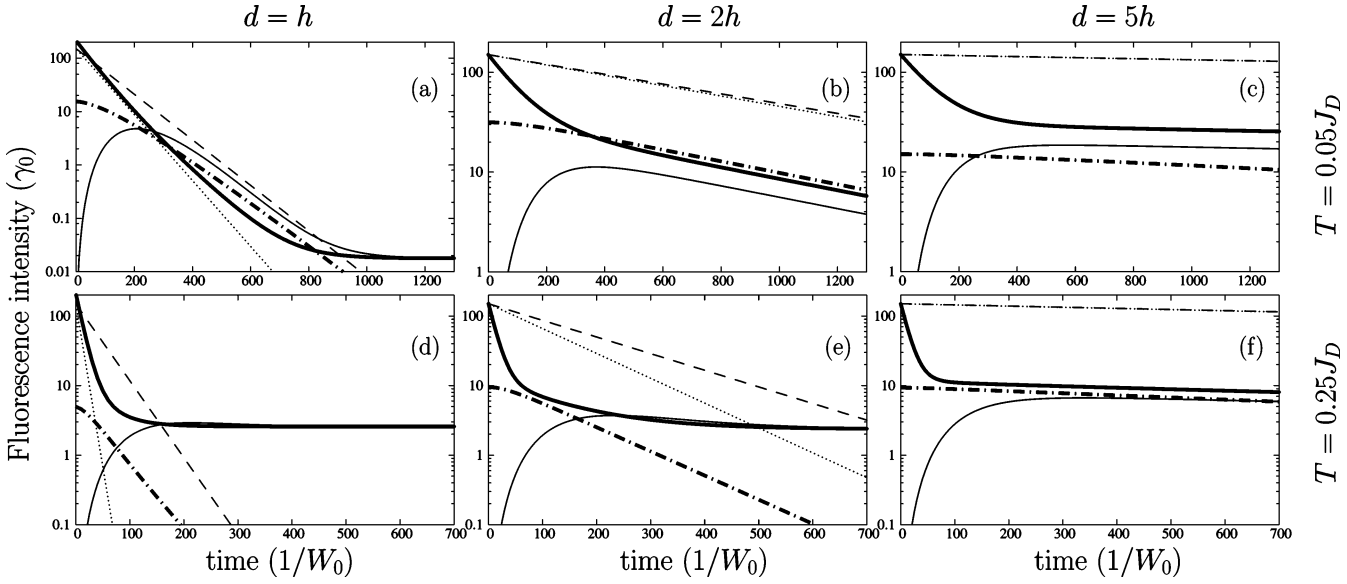

Figure 6. Kinetics of the donor fluorescence for resonant excitation (thick solid curve) and off-resonant excitation (thin solid curve) calculated for various distances ($d/h = 1$, 2, and 5 from left to right) and temperatures ($T = 0.05\ J_D$ and $0.25\ J_D$ for top and bottom rows, respectively). All other parameters as given at the beginning of Section V. The thick dash−dotted curve shows the difference between the acceptor's fluorescence intensity and its thermal equilibrium value (see text). Finally, the straight lines represent the donor decay assuming fast equilibration over the donor band in the nonperturbative case (dashed curve, eq 20) and the perturbative limit (dotted curve, eq 21).

of the donor fluorescence. At $d = h$ (Figure 5a), it is hardly possible to distinguish the two stages; the fluorescence kinetics only exhibits a fast initial drop, almost directly followed by the Boltzmann plateau. The reason is that, for $d \lesssim h$, the bare donor and acceptor bands are strongly mixed (see Figure 3). As a result, the intra- and interband relaxation rates are of the same order, making it impossible to distinguish their signatures in the fluorescence kinetics. We also observe that the intraband relaxation is much more sensitive to changing the temperature than the energy transfer process. This is due to the fact that this relaxation is directly sensitive to the number of thermally accessible dark states in the donor band.

The above statement that the stage II part of the donor kinetics indeed yields a meaningful measure for the energy transfer rate to the acceptor is corroborated by Figure 6, in which for three different separations at two different temperatures, the donor fluorescence kinetics is plotted again (thick solid curves) and is compared to the monoexponential decay obtained through eq 20 at the same temperature (dashed line). In Figure 6b, c, e, and f, stage II can be distinguished, and this part of the kinetics is (roughly) parallel to the monoexponential curve. The agreement deteriorates with decreasing separation d and with growing temperature. In panel (e), stage II already is rather hard to see, and the agreement with the monoexponential curve is only fair.

In panels (a) and (d), stage II cannot be distinguished, and no part of the fluorescence kinetics shows a reasonable agreement with the monoexponential decay line.

From the above, it may be concluded that in the case of strong interchain coupling, under conditions of resonant excitation, the kinetics of the donor fluorescence is not a good tool to determine the energy transfer rate. One may expect that, under these conditions, the acceptor fluorescence yields a better tool because this quantity is influenced less directly by the upward relaxation within the donor band. For this reason, we also plotted in Figure 6 the acceptor fluorescence as a function of time (thick dash−dotted curves). These curves represent $\gamma_{0-}[P_{0-}(t \rightarrow \infty) - P_{0-}(t)]$, where $P_{0-}(t \rightarrow \infty)$ equals the thermal equilibrium value. We observe that, even in the case of strong coupling and high temperature, the acceptor fluorescence indeed seems to be affected less by the initial thermal relaxation part and more directly reflects the energy transfer rate as calculated assuming equilibration (dashed lines).

2. Off-Resonant Excitation. We next turn to the case of off-resonant excitation. To this end, we also plotted in Figure 6 (thin solid curve) the donor fluorescence after the system has been brought (artificially) in the initial state with $P_{k+}(t) = \delta_{k,N/2}$ and $P_{k-}(t) = 0$, i.e., the center state of the donor band is excited. As for the case of resonant excitation, we observe that, at low temperatures and (or) large interchain separations, the kinetics exhibits two stages prior to reaching the Boltzmann plateau. The first stage, intraband relaxation, now manifests itself through the increase of the donor fluorescence from its initial value zero because the donor population needs time to reach the superradiant bottom state of the donor band. We note that, despite the many relaxation steps needed to reach the bottom, for low temperatures, this first stage occurs on the same time scale or even faster than for the case of resonant excitation. As a result, the stage II process, related to the energy transfer, reflects the same time scale as for resonant excitation.

By contrast, at higher temperatures, the distinction between the first and second stage of the kinetics is less clear: there is a more gradual change between the two, which also creates the impression of a longer time scale for the intraband relaxation. We explain this as follows. As near the band center the mixing of donor and acceptor bands is very strong, the intraband and interband relaxation there happen at the same time scale. As a result, off-resonant excitation is followed by very fast distribution of the excitation over donor and acceptor bands, in both of which the population relaxes to the bottom. Thus, as opposed to the case of resonant excitation, the energy transfer problem at the bottom of the band takes place in a situation where a large part of the population already has ended up in the acceptor band. In this situation, the back transfer from the acceptor to the donor, which takes place at temperatures on the order of the band edge detuning Δ, feeds the donor fluorescence after the initial relaxation, which prolongs the time during which the donor fluorescence increases and slows down its overall kinetics. By comparing to the dashed lines in Figure 6, we observe that, at the higher temperatures, no part of the kinetics curve for off-resonant excitation reflects the energy transfer rate calculated through eq 20. Thus, at high temperatures (comparable to Δ or higher), off-resonantly excited donor fluorescence seems not to be a good ruler for the energy transfer rate. At low temperatures, this technique is more useful and then yields the same transfer rate as donor or acceptor fluorescence after resonant excitation of the donor.

Without showing details, we mention that, in the case of off-resonant excitation, the kinetics of the acceptor fluorescence suffers from the interplay between intraband and interband transfer and therefore does not yield a proper tool for measuring the energy transfer rate either.

VI. Summary and Conclusions

We theoretically studied the excitation energy transfer between two linear chains of dye molecules, whose primary excitations are Frenkel excitons. The superradiant band bottoms of both chains were detuned by a value Δ; the chain with the higher (lower) band bottom was considered as the energy donor (acceptor). In addition to electronic interchain interactions, our theory accounts for weak exciton−phonon coupling. Two methods were investigated. In the perturbative method, we used the common approximation of treating the interchain interactions as a perturbation, which also is the basis for the standard FRET formalism. In the nonperturbative approach, we allowed for mixing of the donor and acceptor exciton bands and considered the various phonon-induced relaxation mechanisms in and between these bands to describe the energy transfer process.

By using the perturbative approach, we have confirmed that energy transfer between multichromophoric systems can occur from and toward dipole-forbidden states.[18−24,34] We have focused, however, on two other aspects specific to multichromophoric systems, namely the effects of band mixing and intraband relaxation on the energy transfer. The first has been studied by comparison of the perturbative and the nonperterbative method. Not surprisingly, we find that the perturbative approach loses its validity when the interchain distance decreases (and the interchain interactions grow). The perturbative result for the energy transfer rate then strongly overestimates the exact one that accounts for band mixing. The distance at which the perturbation theory breaks down increases with temperature because the effect of band mixing is larger for the states inside the bands, which get populated upon heating. We also compared our results to the standard FRET theory, which turns out to lose its validity as soon as the interchain separation falls below the chain length (or exciton delocalization length, in case one considers disordered chains).

From our study it turns out that the process of energy transfer between multichromophoric systems is strongly affected by intraband relaxation. This is most obvious in the kinetics of the donor and acceptor fluorescence after pulsed excitation. As these quantities are natural choices for probing energy transfer, it is important to realize that this kinetics does not only reflect the actual transfer process of interest, but also is affected by thermal relaxation inside the donor and acceptor bands. Only if both processes can be separated, due to different time scales, one may extract the energy transfer rate from such experiments. Our results suggest that the best way of determining the transfer rate between two *J*-aggregates is to measure the fluorescence kinetics of the acceptor's *J*-band after resonant excitation of the donor band. Under these conditions, the acceptor's fluorescence intensity grows toward its equilibrium value almost monoexponentially, allowing for a meaningful definition of the transfer rate. We also found that the thus extracted rate agrees well with the transfer rate obtained when assuming equilibration over the donor band. If, because of relaxation to the ground state, measuring the acceptor's equilibrium fluorescence intensity turns out to be a problem, one may also resort to analyzing the decay of the time derivative of this intensity. The first component of that decay should then reflect the transfer rate, while the second reflects the relaxation to the ground state.

We note that, throughout this paper, we have neglected the homogeneous line widths Γ_k of the individual exciton transitions.

Within our model, these widths result from exciton−phonon scattering.[35] It may be estimated that, within the context of excitation energy transfer, these widths may indeed be neglected (i.e., $\Gamma_k \ll J_{kk}^{DA}$) as long as $W_0 \ll 2\pi J_D{}^2/\omega_c$.

The results of this paper were derived by using the simplest possible model of two interacting homogeneous chains with periodic boundary conditions. The same issues of band mixing and intraband relaxation will play an important role for more general systems where one allows for energy and interaction disorder and (or) for different geometries. In fact, all expressions in Sections III and IV also hold for such more general situations, provided that the various wave functions φ_{kn}^{D}, φ_{kn}^{A}, or $\phi_{\mu n}$ as well as the energies E_k^D, E_k^A, or E_μ are replaced by the eigenvectors and eigenenergies of the corresponding exciton Hamiltonian. An example of great interest to analyze next is a pair of concentric cylindrical aggregates. As explained in the Introduction, our model of two parallel linear aggregates was inspired by this experimentally realized situation.[32,33] Varying the distance between both walls in this system is possible by altering molecular side groups and (or) changing the solvent.

Acknowledgment. J.K. thanks Bob Silbey for encouragement and friendship throughout his career. This research is supported by NanoNed, a national nanotechnology program coordinated by the Dutch Ministry of Economic Affairs.

Appendix A: Some Explicit Expressions for Homogeneous Chains

In this Appendix, we present analytical expressions for the probability overlap functions valid for the ordered case.

By substituting the eigenfunctions eq 4 into eq 12, the probability overlap $\mathcal{O}_{kk'}^{X}$ is obtained as

$$\mathcal{O}_{kk'}^{X} = \frac{1}{N} \tag{A1}$$

Likewise, from eqs 7a and 17, we obtain the probability overlap $\mathcal{O}_{\mu\nu}$ (with μ and ν chosen from $(k, +)$ or $(k, -)$) in the form

$$\mathcal{O}_{\mu\nu} = \frac{1}{2N} \begin{cases} 1 + \dfrac{1}{\sqrt{(1+\eta_k)(1+\eta_{k'})}}, & \mu = (k, \pm), \nu = (k', \pm) \\ 1 - \dfrac{1}{\sqrt{(1+\eta_k)(1+\eta_{k'})}}, & \mu = (k, \pm), \nu = (k', \mp) \end{cases} \tag{A2}$$

References and Notes

(1) Förster, Th. *Ann. Phys.* (Leipzig) **1948**, *2*, 55; In *Modern Quantum Chemistry*; Sinanoglu, O., Ed.; Academic: New York, 1965; Part III.
(2) Dexter, D. L. *J. Chem. Phys.* **1953**, *21*, 836.
(3) Ermolaev, V. L.; Bodunov, E. N.; Sveshnikova, E. B.; Shakhverdov, T. A. *Nonradiative Energy Transfer of Electronic Excitation*; Nauka: Leningrad, 1977; in Russian.
(4) Agranovich, V. M.; Galanin, M. D. *Electronic Excitation Energy Transfer in Condensed Matter*; North-Holland: Amsterdam, 1982.
(5) Andrews, D. L.; Demidov, A. A. *Resonance Energy Transfer*; Wiley: Chichester, 1999.
(6) Ermolaev, V. L.; Sveshnikova, E. B.; Bodunov, E. N. *Usp. Fiz. Nauk* **1996**, *166*, 279 (*Phys.-Usp.* **1996**, *39*, 261).
(7) Jang, S.; Jung, Y. J.; Silbey, R. J. *Chem. Phys.* **2002**, *275*, 319.
(8) Kagan, C. R.; Murray, C. B.; Bawendy, M. G. *Phys. Rev. B* **1996**, *54*, 8633.
(9) Crooker, S. A.; Hollingsworth, J. A.; Tretiak, S.; Klimov, V. L. *Phys. Rev. Lett.* **2002**, *89*, 186802.
(10) Wargnier, R.; Baranov, A. V.; Maslov, V. G.; Stsiapura, V.; Artemyev, M.; Pluot, M.; Sukhanova, A.; Nabiev, I. *Nano Lett.* **2004**, *4*, 451.
(11) Javier, A.; Yun, C. S.; Sorena, J.; Strouse, G. F. *J. Phys. Chem. B* **2003**, *107*, 435.
(12) Imamoglu, A.; Awschalom, D. D.; Burkard, G.; DiVincenzo, D. P.; Loss, D.; Sherwin, M.; Small, A. *Phys. Rev. Lett.* **1999**, *83*, 4204.
(13) Biolatti, E.; Iotti, R. C.; Zanardi, P.; Rossi, F. *Phys. Rev. Lett.* **2000**, *85*, 5647.
(14) Holstein, T.; Lyo, S. K.; Orbach, R. In *Laser Spectroscopy of Solids*; Yen, W. M., Selzer, P. M., Eds.; Springer: Berlin, 1981; p 39.
(15) Malyshev, V. A. In *Spectroscopy of Crystals*; Kaplyanskii, A. A., Ed.; Nauka: Leningrad, 1985; p 100, in Russian.
(16) Basiev, T. T.; Malyshev, V. A.; Przhevuskii, A. K. In *Spectroscopy of Solids Containing Rare-Earth Ions*; Kaplyanskii, A. A., Macfarlane, R. M., Eds.; North-Holland: Amsterdam, 1987; p 275.
(17) Xia, S.; Tanner, P. A. *Phys. Rev. B* **2002**, *66*, 214305.
(18) Sumi, H. *J. Phys. Chem. B* **1999**, *103*, 252.
(19) Mukai, K.; Abe, S.; Sumi, H. *J. Phys. Chem. B* **1999**, *103*, 6096.
(20) Scholes, G. D.; Jordanidis, X. J.; Fleming, G. R. *J. Phys. Chem. B* **2001**, *105*, 1640.
(21) Jordanidis, X. J.; Scholes, G. D.; Fleming, G. R. *J. Phys. Chem. B* **2001**, *105*, 1652.
(22) Scholes, G. D. *Annu. Rev. Phys. Chem.* **2003**, *54*, 57.
(23) Jang, S.; Newton, M. D.; Silbey, R. J. *Phys. Rev. Lett.* **2004**, *92*, 218301.
(24) Fleming, G. R.; Scholes, G. D. *Nature* **2004**, *431*, 256.
(25) Shreve, A. P.; Trautman, J. K.; Frank, H. A.; Owens, T. G.; Albrecht, A. C. *Biochim. Biophys. Acta* **1991**, *1058*, 280.
(26) Jimenez, R.; Dikshit, S. N.; Bradforth, S. E.; Fleming, G. R. *J. Phys. Chem.* **1996**, *100*, 6825.
(27) van Oijen, A. M.; Ketelaars, M.; Köler, J.; Aartsma, T. J.; Schmidt, J. *Science* **1999**, *285*, 400.
(28) Wu, H,-M.; Ratsep, M.; Jankowiak, R.; Cogdell, R. J.; Small, G. J. *J. Phys. Chem. B* **1997**, *101*, 7641.
(29) von Berlepsch, H.; Böttcher, C.; Quart, A.; Regenbrecht, M.; Akari, S.; Keiderling, U.; Schnablegger, H.; Dähne, S.; Kirstein, S. *Langmuir* **2000**, *16*, 5908.
(30) von Berlepsch, H.; Böttcher, C.; Quart, A.; Burger, C.; Dähne, S.; Kirstein, S. *J. Phys. Chem. B* **2000**, *104*, 5255.
(31) von Berlepsch, H.; Kirstein, S.; Hania, R.; Didraga, C.; Pužglys, A.; Böttcher, C. *J. Phys. Chem. B* **2003**, *107*, 14176.
(32) Didraga, C.; Pugžlys, A.; Hania, P. R.; von Berlepsch, H.; Duppen, K.; Knoester, J. *J. Phys. Chem. B* **2004**, *108*, 14976.
(33) Pugžlys, A.; Hania, P. R.; Didraga, C.; Malyshev, V. A.; Knoester, J.; Duppen, K. In *Ultrafast Phenomena XIV*; Kobayashi, T., Okada, T., Kobayashi, T., Nelson, K. A., De Silvestri, S., Eds.; Springer Series in Chemical Physics; Springer: Berlin-Heidelberg-New York, 2005; Vol. 79, p 879.
(34) Fukutake, N.; Takasaka, S.; Kobayashi, T. *Chem. Phys. Lett.* **2002**, *361*, 42.
(35) Heijs, D. J.; Malyshev, V. A.; Knoester, J. *Phys. Rev. Lett.* **2005**, *95*, 177402; *J. Chem. Phys.* **2005**, *123*, 144507.
(36) Bednarz, M.; Malyshev, V. A.; Knoester, J. *J. Chem. Phys.* **2002**, *117*, 6200; **2004**, *120*, 3827.
(37) Landau, L. D.; Lifshits, E. M. *Quantum Mechanics*; Pergamon: Oxford, 1965.
(38) Weiss, U. *Quantum Dissipative Systems*; World Scientific: Singapore, 1993.
(39) Kühn, O.; Sundström, V. *J. Chem. Phys. B* **1997**, *107*, 4154.
(40) May, V.; Kühn, O. *Charge and Energy Transfer Dynamics in Molecular Systems*; Wiley-VCH: Berlin, 2000.
(41) Renger, T.; May, V.; Kühn, O. *Phys. Rep.* **2001**, *343*, 137.
(42) Brüggemann, B.; Szenee, K.; Novoderzhkin, V.; van Grondelle, R.; May, V. *J. Phys. Chem. B* **2004**, *108*, 13536.
(43) Bednarz, M.; Malyshev, V. A.; Knoester, J. *Phys. Rev. Lett.* **2003**, *91*, 217401.